Improved Determination of Relativistic Quantities from LLR

Jürgen Müller
Institute for Astronomical and Physical Geodesy, Technische Universität München
80290 Munich, Germany, Email: jxmx@alpha.fesg.tu-muenchen.de

Ken Nordtvedt
Northwest Analysis, 118 Sourdough Ridge Road, Bozeman, Montana 59715, USA

Manfred Schneider
Research Facility for Space Geodesy, Technische Universität München, 80290 Munich, Germany

David Vokrouhlický
Institute of Astronomy, Charles University, V Holešovičkách 8, 18000 Prague 8, Czech Republic

Abstract

Lunar Laser Ranging (LLR) data can be used to determine parameters of the Earth-Moon system (e.g. lunar gravity, tidal parameters) and quantities parametrizing relativistic effects in the solar system. Among the relativistic parameters are those representing secular effects like $\dot{G}/G$ and periodic effects such as the violation of the equivalence principle (EP). Altogether 10 relativistic parameters have been determined, e.g. metric parameters β and γ, the geodetic precession of the lunar orbit, Yukawa coupling constant, the 'preferred frame' parameters α_1 and α_2 and others. Moreover, LLR contributes to the realisation of the International Terrestrial Reference Frame (ITRF) and provides a set of Earth Orientation Parameters (EOP) like UT0 or nutation coefficients.
We give an overview over the prospects of LLR today and its impact for Geodesy and Relativity.

1. Introduction

Lunar Laser Ranging (LLR) inaugurated as one of the first space geodetic techniques. Observations began shortly after the first Apollo 11 manned mission to the Moon in 1969 which deployed a passive retro-reflector on that body's surface. Since then, and continuing, over 12,000 LLR measurements have by now been made of the distance between Earth observatories and lunar reflectors.
As shown in Figures 1 and 2, the range data has not been accumulated uniformly in time; substantial variations in data density exist as function of synodic angle D and sidereal angle S, each of these phase angles represented by 36 bins of 10 degree width.
In Figure 1, data gaps are seen near new Moon (0 and 360 degrees) and full Moon (180 degrees) phases, and asymmetry about quarter Moon (90 and 270 degrees) phases also is exhibited. The former properties of this data distribution are a consequence of operational restrictions, such as difficulties to target 'dark' reflectors, or of excessive background solar illumination noise. But there seems to be less technical necessity for the latter properties (asymmetry about quarter Moon phases). The uneven distribution with respect to the lunar sidereal angle shown in Figure 2 represents the increased difficulty of making observations from northern hemisphere observatories to the Moon when it is located over the southern hemisphere.
It is possible to construct so-called 'worth functions' which quantify the improved precision for a particular model parameter which results from an observation made at a particular epoch (for details see Nordtvedt (1998) and also in these proceedings). In particular, he finds that new observations made on the new Moon side of quarter Moon phase will have dramatically higher value in improving precision of fit for the Equivalence Principle parameter η as compared to new observations made on the full Moon side of quarter Moon phases. And this preference grows strongly as the observation epoch approaches new Moon phase. This situation is a result of the past practice of preferentially observing on the full Moon side of quarter Moon.

It would also be advantageous to increase the LLR ranging data during periods when the Moon is in the southern hemisphere. It is possible that the Japanese SELENE II mission to the Moon could be helpful in this respect; its deployment of an active laser transponder could allow the new generation, mobile laser ranging systems to participate in LLR.

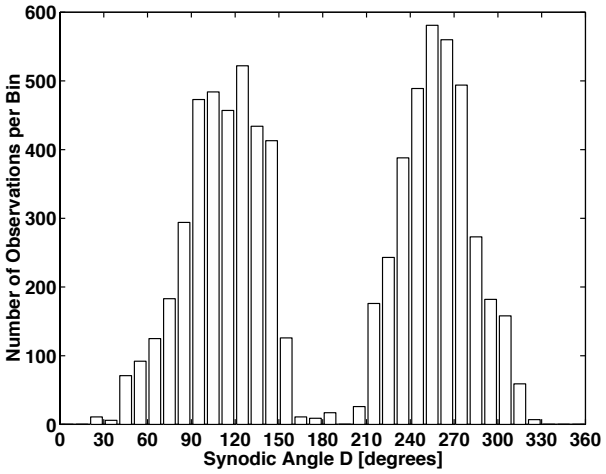

Figure 1: Data distribution as a function of the synodic angle D.

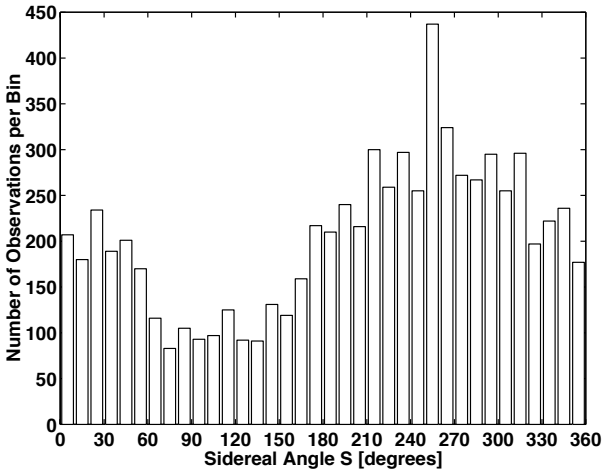

Figure 2: Data distribution as a function of the sidereal angle S.

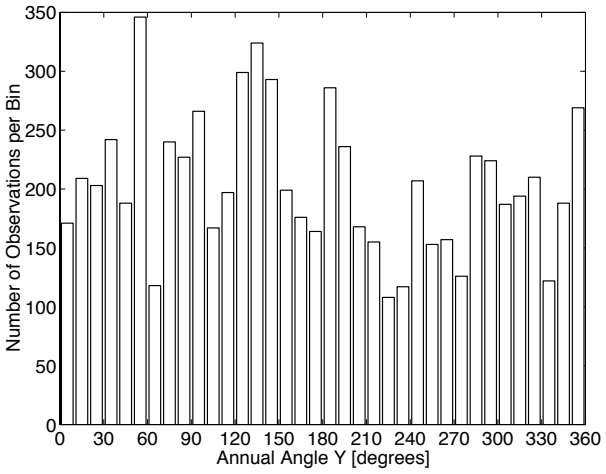

Figure 3: Data distribution as a function of the annual angle Y.

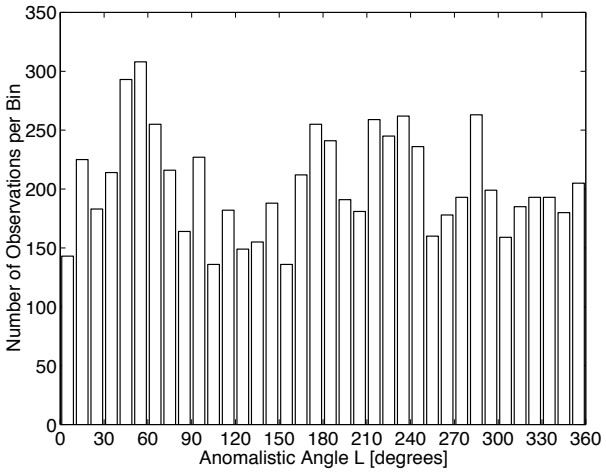

Figure 4: Data distribution as a function of the anomalistic angle L.

For comparison, Figures 3 and 4 show the data distribution as function of the annual phase Y and anomalistic phase L. No large data density variations are found, though perhaps slight variations over the year are present due to seasonal change of length-of-night in the northern hemisphere, or seasonal weather variations which sensitively affect chances for optical ranging[1].
While measurement precision for all model parameters benefit from the ever-increasing improvement in precision of individual range measurements (which now is about 1 cm!), some parameters of scientific interest, such as time variation of NEWTON's coupling parameter $\dot{G}/G$ or precession rate of lunar perigee, particularly benefit from the long time period (30 years and growing) of range measurements.

[1]As an optical technique, LLR is strongly dependent of weather conditions which lead to further inhomegeneities in the distribution of measurements. Due to the large distance the energy balance for each laser observation looks very bad: only one photon out of 10^{19} transmitted ones finds its way back to the receiver.

A year before the Apollo 11 mission, it was theoretically shown that LLR could perform a useful new test of general relativity theory by means of testing the equality of Earth and Moon's gravitational acceleration rates toward the Sun (NORDTVEDT, 1968a and 1968b). The possibility to test EINSTEIN's theory, was one important reason for setting up the LLR experiment.
In the seventies LLR was the only space technique other than classical astronomy for determining Earth orientation parameters. Today LLR still competes with other space geodetic techniques, and because of large improvements in ranging precision (30 cm in 1969 to 1 cm today), it now serves as one of the strongest tools in the solar system for testing general relativity. It contributes to the combined EOP solutions performed by the International Earth Rotation Service (IERS) and to the realization of the International Terrestrial Reference Frame (ITRF).

2. LLR Model

Using EINSTEIN's general relativity theory of gravity, a model complete up to first post-NEWTONian $(1/c^2)$ level has been developed for computing the LLR observables — the roundtrip travel times of laser pulses between stations on the Earth and passive reflectors on the Moon (see e.g. MÜLLER et al., 1996 or MÜLLER & NORDTVEDT, 1998 and the references therein). This last year the model has been improved by including effects like ocean loading, solar radiation pressure, rotation rate of the Earth and its obliquity precession, and by better representing other parts of the model like solid Earth tides, orbital perturbations due to the asteroids etc. Useful suggestions were found in the IERS conventions (1996) e.g. for modelling the tidally driven diurnal and semidiurnal UT1 variations, and the solid Earth tides.
Using such a many-parameter (about 170) model for the description of the Earth-Moon motion in the solar system, its dynamics can then be integrated. Two groups of parameters are determined by a weighted least-squares fit of the observations. The first group are so-called 'NEWTONian' parameters such as

- geocentric coordinates of four stations (including Wettzell where only a few observations are available); optional drift rates of the corresponding continental plates;
- a set of Earth's orientation parameters (luni-solar precession constant, nutation coefficients of the 18.6 years period, Earth's rotation UT0 and variation of latitude by polar motion);
- selenocentric coordinates of four retro-reflectors;
- rotation of the Moon for one initial epoch (physical librations);
- orbit (position and velocity) of the Moon for this epoch;
- orbit of the Earth-Moon system about the Sun for one epoch;
- mass of the Earth-Moon system times the gravitational constant;
- the lowest mass multipole moments of the Moon;
- lunar Love number and a rotational energy dissipation parameter;
- lag angle indicating the lunar tidal acceleration responsible for the increase of the Earth-Moon distance (and the slow down of Earth's angular velocity);
- quadrupole moment of the Sun $J_2^{\odot}$ which could also be added to the second group because it contributes to the anomalous perihelion advance of Mercury.

The second group of parameters serve in models for the plausible modifications of general relativity theory which can be tested by LLR (these parameter values for general relativity are given in brackets)

- geodetic deSITTER precession $\Omega_{\rm dS}$ (proportional to $\gamma + 1/2$) of the lunar orbit ($\simeq 1.92''/cy$);

- metric parameters γ (= 1) scaling motional and β (= 1) scaling non-linearity corrections in body equations of motion (EINSTEIN-INFELD-HOFFMANN equations) and in the light time equation[2];
- strong EP parameter $\eta = 4\beta - 3 - \gamma$ (= 0) in metric theories, and weak EP parameter δ (= 0) for non-metric situations;
- time variation of the gravitational coupling parameter $\dot{G}/G$ (= 0 yr^{-1}) which is important for the unification of the fundamental interactions;
- coupling constant α (= 0) of Yukawa potential for the Earth-Moon distance which corresponds to a test of NEWTON's inverse square law;
- combination of parameters $\zeta_1 - \zeta_0 - 1$ (= 0) derived in the MANSOURI and SEXL (1977) formalism indicating a violation of special relativity (there: LORENTZ contraction parameter $\zeta_1 = 1/2$, time dilation parameter $\zeta_0 = -1/2$);
- EP-violating coupling of normal matter to 'dark matter' at the galactic center;
- α_1 (= 0) and α_2 (= 0) which parameterize 'preferred frame' effects in metric gravity.

Most relativistic effects produce periodic perturbations of the Earth-Moon range

$$\Delta r_{EM} = \sum_{i=1}^{n} A_i \cos(\omega_i \Delta t + \Phi_i). \tag{1}$$

A_i, ω_i, *and* ϕ_i are the amplitudes, frequencies, and phases, respectively, of the various perturbations. Some example periods of perturbations important for the measurement of various parameters are given in Table 1.[3]
These properties (relativistic phenomena show up with typical periods) can be used to identify and separate the different effects and to determine corresponding parameters.

Table 1: Typical periods of some relativistic quantities.

Parameter	Typical Periods
η	synodic ($29^d\ 12^h\ 44^m\ 2.9^s$)
ζ_1-ζ_0-1	annual (365.25^d)
$\delta g_{galactic}$	sidereal ($27^d\ 7^h\ 43^m\ 11.5^s$)
α_1	sidereal, annual, sidereal - 2*annual, anomalistic ($27^d\ 13^h\ 18^m\ 33.2^s$) $\pm$ annual, synodic
α_2	2*sidereal, 2*sidereal - anomalistic, nodal (6798^d)
$\dot{G}/G$	secular + emerging periodic

3. Results

The global adjustment of the model by least-squares-fit procedures gives improved values for the estimated parameters and their formal standard errors, while consideration of parameter correlations

[2]However, the light propagation effect contributes only little to the determination of γ because its constant part is completely absorbed by scaling $GM_{Earth+Moon}$ or the semimajor axis of the Earth-Moon orbit about the Sun.

[3]Don't misuse the given designations as formulae for the computation of the corresponding periods, e.g. the period 'sidereal - 2*annual' has to be calculated as $1/(1/27.32^d - 2/365.25^d) \approx 32.13^d$.
'secular + emerging periodic' means the changing orbital frequencies induced by $\dot{G}/G$ are starting to become better signals than the secular rate of change of the Earth-Moon range in LLR. Therefore a more rapid improvement in measuring this parameter can be expected in coming years.

obtained from the covariance analysis and of model limitations lead to more 'realistic' errors. For example, we describe the error analysis for the EP-violating amplitude $A_D = 12.8\ \eta$ [m]

$$\Delta r_{em} = A_D \cos(D). \tag{2}$$

The formal fit of $A_D = 1.0 \pm 0.2$ cm indicates there is an unmodelled synodic signal in the data, but not necessarily of relativistic origin. Incompletely modelled solid Earth tides, ocean loading or geocenter motion, and uncertainties in values of fixed model parameters lead to a total realistic error of $\boldsymbol{\sigma_{A_D}}$**(realistic) = 1.1 cm** resp. $\eta \leq 9 \cdot 10^{-4}$. If this result is interpreted as a test of the weak form of the EP (composition dependence of free fall rates), the silicate Moon and iron-cored Earth falling differently toward the Sun then yield, after taking into account the Earth core fraction

$$\delta_{S,I} \ \simeq \ 1 \cdot 10^{-12} \tag{3}$$

with $\delta_{S,I}$ being the fractional difference in free fall rates for these two materials.

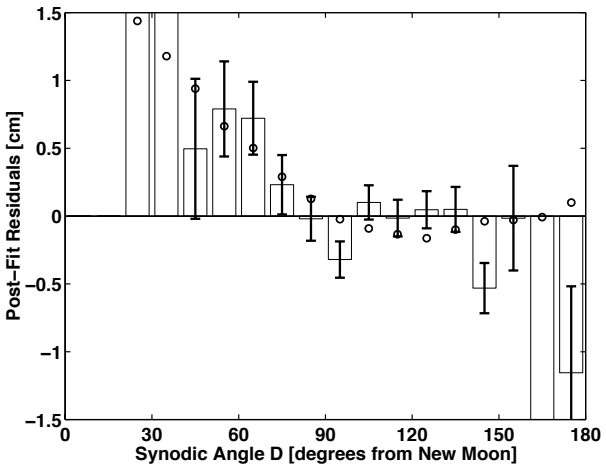

Figure 5: Synodic bins. The 'o' show the effect of a '1cm $\cos(D)$' signal.

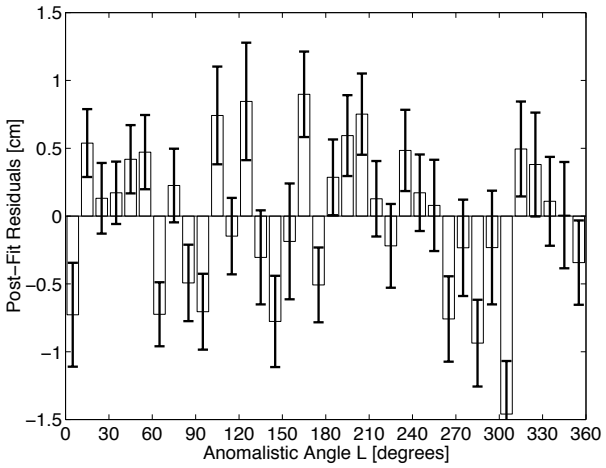

Figure 6: Anomalistic bins of the post-fit residuals.

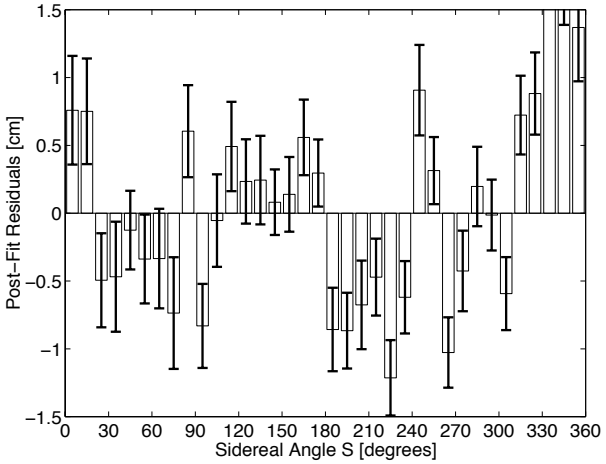

Figure 7: Sidereal bins of the post-fit residuals.

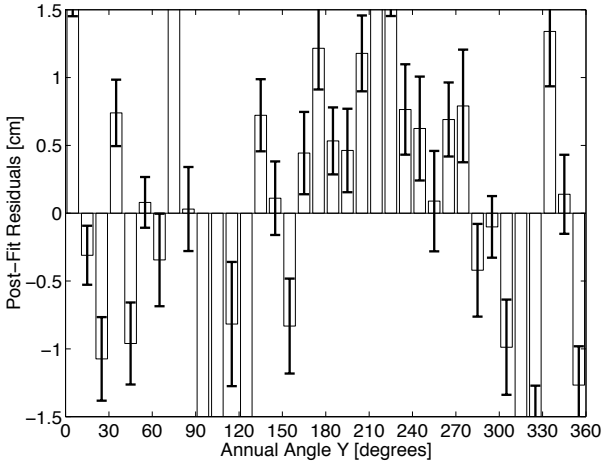

Figure 8: Annual bins of the post-fit residuals.

This fit has been investigated more deeply by constructing and plotting 'synodic bin-averaged' post-fit residuals as function of the synodic angle D (measured from nearest new Moon phase). As shown in Figure 5, each bin bar represents an average of hundreds of post-fit range residuals with synodic

angle within the 10 degree width of each bin, but otherwise spread in time over the total years of the experiment. The plotted errors for each average value reflect only the observer-supplied uncertainties of the original normal points. The curve of markings 'o' indicate the changes of these bin averages which resulted when an artificial signal '1 cm cos(D)' was added to the actual LLR residuals. It supports the interpretation that there is an unmodelled signal of 1 cm characteristic size left in the data and it also confirms the realistic error of about 1.1 cm (see also MÜLLER & NORDTVEDT, 1998). Similar investigations have been performed for other relativistic parameters. For example, non-zero values for the 'preferred frame' parameters α_1 and α_2 will produce signals which are superpositions of sidereal, annual, synodic and anomalistic frequencies (see Table 1). Looking at the binned post-fit residuals in Figures 5 - 8, obtained prior to any fits for 'preferred frame' effects, no systematic signals other than the previously discussed synodic signal are visible, and therefore no significant non-zero values for α_1 and α_2 are expected. These parameters have been estimated in two different ways: 1) we have obtained the partials for these two parameters by analytic means and added such signals to the parameterized model, and 2) we added the actual acceleration terms associated with these parameters to the equations of motion and generated the partials by numerical integration (see MÜLLER et al., 1996 and MÜLLER et al., 1998).
The resulting formal error values for the parameters are listed in Table 2 along with realistic errors obtained as previously described.

Table 2: Error analyis of the 'preferred frame' parameters α_1 and α_2.

	σ_{α_1}	σ_{α_2}
effect of inaccurate modelling resp. use of inaccurate model parameters	$8{\cdot}10^{-5}$	$2.4{\cdot}10^{-5}$
formal (1σ) error	$2{\cdot}10^{-5}$	$0.4{\cdot}10^{-5}$
realistic error	$\mathbf{9 \cdot 10^{-5}}$	$\mathbf{2.5 \cdot 10^{-5}}$

Final results for all relativistic parameters are shown in Table 3. The realistic errors are comparable with those obtained in other recent investigations (see e.g. WILLIAMS et al., 1996).

Table 3: Determined values for the relativistic quantities and their realistic errors.

Parameter	Results
diff. geod. prec. $\Omega_{\rm GP}$ - $\Omega_{\rm deSit}$ ["/cy]	$(-2 \pm 10) \cdot 10^{-3}$
metric par. $\gamma - 1$	$(4 \pm 5) \cdot 10^{-3}$
metric par. $\beta - 1$	$(-1 \pm 4) \cdot 10^{-3}$
equiv. principle par. η	$(8 \pm 9) \cdot 10^{-4}$
time var. grav. const. $\dot{G}/G$ [yr^{-1}]	$(3 \pm 5) \cdot 10^{-12}$
Yuk. coupl. const. $\alpha_{\lambda=4{\cdot}10^5\,\rm km}$	$(2 \pm 2) \cdot 10^{-11}$
spec. relativi. $\zeta_1 - \zeta_0 - 1$	$(-5 \pm 12) \cdot 10^{-5}$
infl. of dark matter $\delta g_{galactic}$ [cm/s^2]	$(4 \pm 4) \cdot 10^{-14}$
'preferred frame' effect α_1	$(-8 \pm 9) \cdot 10^{-5}$
'preferred frame' effect α_2	$(-1.2 \pm 2.5) \cdot 10^{-5}$

Although we concentrate our investigations to determine relativistic quantities, LLR data are used to compute new solutions of EOPs (UT0 and variation of latitude by polar motion) each year covering the whole period of observations since 1970. The accuracy for UT0 is about 50 μs nowadays which is in agreement with other space geodetic techniques. The results are submitted to the IERS where they

are combined to a global solution. The same is valid for a set of station coordinates which are estimated simultaneously and submitted to the IERS to contribute to the realisation of the international terrestrial reference frame ITRF.
A similar error analysis has been performed for the 'NEWTONian' parameters; these results can be received from the author J. MÜLLER on request.
In 1998 the International Laser Ranging Service (ILRS) has been established to improve the international cooperation of the various laser centers and to better pre-process the laser-related products for the scientific community. Our group contributes to the ILRS as Lunar Analysis Center.

4. Conclusion

For the IERS, LLR contributes to the realisation of the International Terrestrial Reference Frame and to combined solutions of Earth Orientation Parameters.
Additionally, LLR has become a technique for measuring a variety of relativistic gravity parameters with unsurpassed precision. No definitive violation of the predictions from general relativity are found, though evidence of modelling inadequacies are present in the synodically plotted residuals. Both the weak and strong forms of the EP are verified, while strong empirical limitations on presence of inverse square law violation, time variation of G, and preferred frame effects are also obtained.
LLR continues as an active program, and it can remain as one of the most important tools for testing EINSTEIN's general relativity theory of gravitation if appropriate observations strategies are adopted and if the basic LLR model is further extended and improved down to the millimeter level of accuracy.

References

IERS Conventions (1996). IERS Technical Note 21 (ed. D.D. McCARTHY).

MANSOURI R.M. and SEXL R.U. (1977). *A test theory of Special Relativity.* General Relativity and Gravitation, 8, No. 7, 497-513 (*Part I*); No. 7, 515-524 (*Part II*); No. 10, 809-814 (*Part III*).

MÜLLER J. and NORDTVEDT K. (1998). *Lunar laser ranging and the equivalence principle signal.* Physical Review D, 58, 062001.

MÜLLER J., NORDTVEDT K. and VOKROUHLICKÝ D. (1996). *Improved constraint on the α_1 PPN parameter from lunar motion.* Physical Review D, 54, R5927-R5930.

MÜLLER J., NORDTVEDT K. and VOKROUHLICKÝ D. (1998). *Gravitation anisotropy bounds from lunar motion: α_2 PPN parameter.* Physical Review D, accepted.

NORDTVEDT K. (1968a). *Equivalence principle for massive bodies. II. Theory.* Physical Review, 169, 1017-1025.

NORDTVEDT K. (1968b). *Testing relativity with laser ranging to the Moon.* Physical Review, 170, 1186.

NORDTVEDT K. (1998). *Optimizing the observation schedule for tests of gravity in lunar laser ranging and similar experiments.* Classical and Quantum Gravity, 15, No. 11, 3363.

NORDTVEDT K. (1999). *Optimizing the observation schedule in LLR and similar experiments.* These Proceedings.

WILLIAMS J.G., NEWHALL X.X. and DICKEY D.O. (1996). *Relativity parameters determined from lunar laser ranging.* Physical Review D, 53, 6730.